Steel and Composite Structures, *Vol. 17, No. 6 (2014) 867-890*
DOI: http://dx.doi.org/10.12989/scs.2014.17.6.867

Nonlinear bending analysis of laminated composite stiffened plates

Shuvendu N. Patel *

Department of Civil Engineering, BITS Pilani, Pilani Campus, Pilani - 333031, Rajasthan, India

(*Received November 11, 2013, Revised July 27, 2014, Accepted August 23, 2014*)

Abstract. This paper deals with the geometric nonlinear bending analysis of laminated composite stiffened plates subjected to uniform transverse loading. The eight-noded degenerated shell element and three-noded degenerated curved beam element with five degrees of freedom per node are adopted in the present analysis to model the plate and stiffeners respectively. The Green-Lagrange strain displacement relationship is adopted and the total Lagrangian approach is taken in the formulation. The convergence study of the present formulation is carried out first and the results are compared with the results published in the literature. The stiffener element is reformulated taking the torsional rigidity in an efficient manner. The effects of lamination angle, depth of stiffener and number of layers, on the bending response of the composite stiffened plates are considered and the results are discussed.

Keywords: degenerated shell element; degenerated curved beam element; nonlinear analysis; green-lagrange nonlinearity; stiffened plate and laminated composite

1. Introduction

With the increased application of fiber reinforced composites in various fields, research on their behaviour for different structural form has also increased. Most commonly used structural forms are plates, used in aircraft, ship and automotive industries. The performance, i.e., strength/stiffness to weight ratio of the plates is enhanced by adopting suitable stiffened forms. The advanced mechanical properties of composite materials have resulted in large weight saving, and the use of stiffeners further enhance the weight saving. The composite material along with the use of stiffeners, have given flexibility in designing an efficient component, at the same time it requires a complex mathematical model to analyze their behaviour. As the structural components become very thin with the use of composite material and again with the use of stiffeners, they become susceptible to large deformation (Polat and Ulucan 2007, Zhang and Kim 2006). At higher loads the transverse deflection of plate is large compared to its thickness. The bending and stretching coupling comes into play and the load deflection behaviour becomes non-linear. At large deflection level, membrane stresses are produced which give additional stiffness to the structure. So a large deflection analysis provides accurate responses.

*Corresponding author, Assistant Professor, E-mail: shuvendu@pilani.bits-pilani.ac.in

http://www.techno-press.org/?journal=scs&subpage=8 ISSN: 1229-9367 (Print), 1598-6233 (Online)

Sheikh and Mukhopadhyay (2000) have performed the geometric nonlinear analysis of isotropic stiffened plates by the spline finite strip method. von Karman's nonlinear plate theory is adopted by them and the formulation is made in total Lagrangian coordinate system.

Koko and Olson (1991) used a super-element approach for the large deflection and elastoplastic analyses of orthogonally stiffened plates. The super-elements are designed to contain all the basic mode of deformation so that only one plate element per bay and one beam element per span are needed to analyze a stiffened structure, therefore reducing the storage requirement and solution time. The geometrically non-linear analysis of isotropic stiffened plates with arbitrarily oriented stiffener was reported by Rao *et al*. (1993). The authors presented the finite element static analysis of the large deflection response of isotropic stiffened plates using an isoparametric quadratic stiffened plate bending element. The stiffened element was a development of the linear formulation presented by Mukhopadhyay and Satsangi (1984). The authors excluded the contribution of the stiffener non-linearities in their formulation. Paik and Lee (2005) have developed an analytical method to carry out the elastic-plastic large deflection analysis of stiffened panels under combined biaxial compression/tension, biaxial in-plane bending, edge shear, and lateral pressure loads. They have used the Galerkin method in their formulation. Sapountzaki and Dikaros (2012a) have performed a general solution to the geometrically nonlinear analysis of plates stiffened by arbitrarily placed parallel beams of arbitrary monosymmetric cross sections with a deformable connection subjected to arbitrary loading. The plate-beam structure is assumed to undergo moderate large deflections and the nonlinear analysis is carried out by retaining the nonlinear terms in the kinematical relationships. According to the proposed model, the stiffening beams are isolated from the plate by sections in the lower outer surface of the plate under the hypothesis that the plate and the beams can slip in all directions of the connection without separation and the arising tractions in all directions at the fictitious interfaces are taken into account. The same authors (Sapountzaki and Dikaros 2012b) have also carried out the geometric nonlinear analysis of stiffened plates without the deformable connection.

The large deflection analysis of un-stiffened composite plates has been extensively reviewed in the paper by Chia (1988). The literature dealing with the flexural behaviour of laminated composite stiffened plates is few and mostly restricted to small deflection. Turvey (1983) has analyzed the uniformly loaded ring-stiffened composite stiffened plates for large deflection. In his modeling, the effect of stiffener in the plate has been incorporated by considering statically equivalent local body forces acting on the plate. The large deflection equations have been solved by finite difference scheme. Liao and Reddy (1990) have investigated the large deflection behaviour of composite stiffened plates and shells by the finite element method. They have used degenerated three dimensional shell elements and associated curved beam elements which have been derived from the degenerated elements by imposing appropriate kinematic constraints. The incremental equations of motion developed using the principle of virtual displacement of a continuum and the total Lagrangian concept have been solved by the Newton-Raphson iteration procedure. The experimental investigation on the flexural behaviour of composite stiffened plate in the nonlinear range has been carried out by Hyer *et al*. (1990). They have used the STAGS (Almroth and Brogan 1978) computer code to compare the experimental results with the analytical ones. STAGS models the stiffened plate as shell branches. Chattopadhyay *et al*. (1995) have performed the large deflections analysis of laminated composite stiffened plates using an eight noded isoparametric element. The element formulation is based on Reissner–Mindlin's hypothesis with a total Lagrangian description of motion. The nonlinear equilibrium equations are solved by the Newton-Raphson iteration procedure. Goswami and Mukhopadhyay (1995) have analyzed the

eccentrically stiffened composite shells for the first time in the literature. They have used the 9-noded curved Lagrangian element stiffened with laminated stiffeners in their formulation. They have not reported any plate results in this paper. Kolli and Chandrashekhara (1997) have presented the static and dynamic analysis of eccentrically stiffened laminated plates. In the formulation they have considered the von Kamran kinematic relations of plate and stiffener. This formulation can analyze thin and thick laminated stiffened plates. They have used nine-noded isoparametric quadrilateral elements for the plate and three-noded isoparametric beam elements for the stiffeners. Ojeda *et al*. (2007) have carried out the large deflection finite element analysis of isotropic and composite plates with arbitrary orientated stiffeners. The large deflection analysis of laminated composite stiffened plates without stiffeners have been carried out by Cetkovic and Vuksanovic (2011a, b) using layer wise displacement model. With the layerwise displacement field, nonlinear Green-Lagrange small strain large displacements relations (in the von Karman sense) and linear elastic orthotropic material properties for each lamina, the 3D elasticity equations are reduced to 2D problem and the nonlinear equilibrium integral form is obtained. The resulting equations are solved by MATLAB computer program. Dash and Singh (2010) have performed the geometrically nonlinear bending analysis of laminated composite un-stiffened plate by finite element method.

From the literature it is revealed that the works reported by the earlier investigators in the nonlinear bending behaviour of laminated composite stiffened plates are few. Still there exist a lot of scope to study the large deflection behaviour of the composite stiffened plates, as the thin composite structural elements are highly susceptible to large deformation. In this paper the emphasis has been given in the formulation of shell element and the stiffener element with the Green-Lagrange strain displacement relationship. The formulation of the stiffener is efficient. The nonlinear bending analysis of laminated stiffened plate subjected to uniform transverse loading is carried out. The total Lagrangian approach is taken in the formulation of the nonlinear equlibrium equations. The resulting nonlinear equations are solved by the Newton-Raphson iteration technique along with the incremental method. The effects of lamination angle, depth of stiffener and number of layers, on the bending response of the composite stiffened plates are considered and the results are discussed.

2. Formulation

The plate skin and the stiffeners are modeled discretely. The plate is modeled with Ahmad *et al*.'s (1970) degenerated shell element with Green-Lagrange strain displacement relationship. The element contains five degree of freedom per node, θ_z is neglected. Shear correction factor of 5/6 is adopted in the stress-strain relationship for transverse shear stresses. A three noded degenerated curved beam element with five degree of freedom per node is taken to model the stiffeners. As the in-plane rigidity of the plate is very high the sixth d.o.f. θ_z in the beam element is also neglected, as the bending of stiffener in the in-plain direction of the plate skin is insignificant. To consider the torsional rigidity of the beam adequately, a torsional correction factor is introduced in the formulation of the stiffener. The formulation of stiffener element is also based on the degeneration of the three dimensional solid element following the basic concept of degeneration of the shell element. The detail formulations of the shell element and stiffener element are presented below.

2.1 Shell element

The formulation of the shell element is based on the basic concept of Ahmad *et al*. (1970), where the three-dimensional solid element used to model the shell is degenerated with the help of certain extractions obtained from the consideration that the dimension across the shell thickness is sufficiently small compared to other dimensions. The detail derivation of this element for isotropic case is available in the literature (Ahmad *et al*. 1970, Zienkiewicz 1977, Rao 1999).

The element has a quadrilateral shape having eight nodes as shown in Fig. 1(a) where the external top and bottom surfaces of the element are curved with linear variation across the shell thickness. Fig. 1(b) shows the global Cartesian and local co-ordinate system at any node *i*. The geometry of the element can be nicely represented by the natural coordinate system (ξ, η and ζ) where the curvilinear coordinates (ξ - η) are in the shell mid-surface while ζ is linear coordinate in the thickness direction. According to the isoparametric formulation, these coordinates (ξ, η and ζ) will vary from –1 to +1 on the respective faces of the element. The relationship (Eq. (1)) between the global Cartesian coordinates (x, y and z) at any point of the shell element with the curvilinear coordinates holds good. This is the geometry of an element, which is described by the coordinates of a set of points taken at the top and bottom surfaces, where the line joining a pair of points (i_{top} and i_{bottom}) is along the thickness direction i.e., normal to the mid-surface at the ith node point. The line joining the top and bottom points is the normal vector (V_{3i}) at the nodal point i.

$$\begin{Bmatrix} x \\ y \\ z \end{Bmatrix} = \sum_{i=1}^{8} N_i(\xi,\eta)\frac{1+\zeta}{2}\begin{Bmatrix} x_i \\ y_i \\ z_i \end{Bmatrix}_{top} + \sum_{i=1}^{8} N_i(\xi,\eta)\frac{1-\zeta}{2}\begin{Bmatrix} x_i \\ y_i \\ z_i \end{Bmatrix}_{bottom} \tag{1}$$

where N_i are the quadratic serendipity shape functions in (ξ - η) plane of the two- dimensional element.

Eq. (1) may be rewritten in terms of mid-surface nodal coordinates with the help of unit nodal vectors (v_{3i}) along the thickness direction as

$$\begin{Bmatrix} x \\ y \\ z \end{Bmatrix} = \sum_{i=1}^{8} N_i(\xi,\eta)\begin{Bmatrix} x_i \\ y_i \\ z_i \end{Bmatrix} + \sum_{i=1}^{8} N_i(\xi,\eta)\frac{\zeta \times h_i}{2}\begin{Bmatrix} l_{3i} \\ m_{3i} \\ n_{3i} \end{Bmatrix} \tag{2}$$

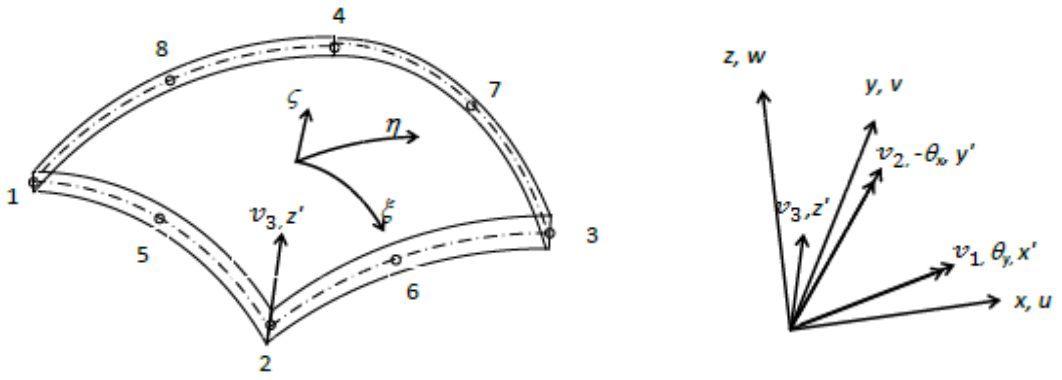

Fig. 1 (a) Eight-noded quadrilateral degenerated shell element in curvilinear co-ordinates; (b) Global Cartesian co-ordinate (x, y and z) and local co-ordinate system at any node i

where, l_{3i},m_{3i} and n_{3i} are direction cosines of the nodal vector (V_{3i}), i.e., components of unit nodal vectors (v_{3i}), v_{3i} is the unit vector along (V_{3i}) direction, h_i is the thickness at node i.

Two orthogonal tangential vectors V_{2i} and V_{1i} are formed at the node i which are normal to V_{3i} vector. The two tangential vectors V_{2i} and V_{1i} not necessarily follow ξ and η directions. The unit vectors along V_{2i} and V_{1i} directions are v_{2i} and v_{1i}. The local co-ordinates x', y' and z' are directed along V_1, V_2 and V_3 directions respectively. The directions cosines of x', y' and z' and V_1, V_2 and V_3 are same as the components of unit vectors v_1, v_2 and v_3. The displacement u, v and w are along the global coordinates x, y and z directions. Similarly the local displacement components u', v' and w' are along the local coordinates x', y' and z' directions. The rotations of the mid surface normal θ_x and θ_y are taken about the local coordinates y' and x' or v_2 and v_1 directions respectively.

The displacement field (Eq. (3)) of a point within the element can be defined with the help of three mid surface nodal translational displacement(u_i, v_i and w_i) along the global Cartesian co-ordinates directions and two rotational components θ_{xi} and θ_{yi} about the local coordinates y' and x' directions.

$$\begin{Bmatrix} u \\ v \\ w \end{Bmatrix} = \sum_{i=1}^{8} N_i(\xi,\eta) \begin{Bmatrix} u_i \\ v_i \\ w_i \end{Bmatrix} - \sum_{i=1}^{8} N_i(\xi,\eta) \frac{\zeta \times h_i}{2} \begin{bmatrix} l_{1i} & l_{2i} \\ m_{1i} & m_{2i} \\ n_{1i} & n_{2i} \end{bmatrix} \begin{Bmatrix} \theta_{xi} \\ \theta_{yi} \end{Bmatrix} = [N_D]\{d\} \tag{3}$$

where, l_{1i},m_{1i} and n_{1i} are direction cosines of the nodal vector (V_{1i}), i.e., components of v_{1i}, l_{2i}, m_{2i} and n_{2i} are direction cosines of the nodal vector (V_{2i}), i.e., components of v_{2i}, and $\{d\}$ is nodal displacement vector

$$\{d\} = [u_1\ v_1\ w_1\ \theta_{x1}\ \theta_{y1}\ u_2\ u_2 - - - - \theta_{x8}\ \theta_{y8}]^T \tag{4}$$

The strain displacement relationship with Green-Lagrange strain of the element in local co-ordinate system (x'-y'-z') can be expressed as

$$\{\varepsilon'\} = \begin{Bmatrix} \varepsilon'_x \\ \varepsilon'_y \\ \gamma_{x'y'} \\ \gamma_{y'z'} \\ \gamma_{x'z'} \end{Bmatrix} = \begin{Bmatrix} \dfrac{\partial u'}{\partial x'} \\ \dfrac{\partial v'}{\partial y'} \\ \dfrac{\partial u'}{\partial y'} + \dfrac{\partial v'}{\partial x'} \\ \dfrac{\partial v'}{\partial z'} + \dfrac{\partial w'}{\partial y'} \\ \dfrac{\partial u'}{\partial z'} + \dfrac{\partial w'}{\partial x'} \end{Bmatrix} + \begin{Bmatrix} \dfrac{1}{2}\left(\left(\dfrac{\partial u'}{\partial x'}\right)^2 + \left(\dfrac{\partial v'}{\partial x'}\right)^2 + \left(\dfrac{\partial w'}{\partial x'}\right)^2\right) \\ \dfrac{1}{2}\left(\left(\dfrac{\partial u'}{\partial y'}\right)^2 + \left(\dfrac{\partial v'}{\partial y'}\right)^2 + \left(\dfrac{\partial w'}{\partial y'}\right)^2\right) \\ \left(\dfrac{\partial u'}{\partial x'} \times \dfrac{\partial u'}{\partial y'} + \dfrac{\partial v'}{\partial x'} \times \dfrac{\partial v'}{\partial y'} + \dfrac{\partial w'}{\partial x'} \times \dfrac{\partial w'}{\partial y'}\right) \\ \left(\dfrac{\partial u'}{\partial y'} \times \dfrac{\partial u'}{\partial z'} + \dfrac{\partial v'}{\partial y'} \times \dfrac{\partial v'}{\partial z'} + \dfrac{\partial w'}{\partial y'} \times \dfrac{\partial w'}{\partial z'}\right) \\ \left(\dfrac{\partial u'}{\partial x'} \times \dfrac{\partial u'}{\partial z'} + \dfrac{\partial v'}{\partial x'} \times \dfrac{\partial v'}{\partial z'} + \dfrac{\partial w'}{\partial x'} \times \dfrac{\partial w'}{\partial z'}\right) \end{Bmatrix} \tag{5}$$

$$\{\varepsilon'\} = \{\varepsilon'_0\} + \{\varepsilon'_{nl}\} \tag{6}$$

After performing number of operations using Eqs. (2) and (3) we can write

$$\{\varepsilon'\} = [B'_0]\{d\} + \frac{1}{2}[B'_{nl}]\{d\} \tag{7}$$

$$\{\varepsilon'\} = [B'_0]\{d\} + \frac{1}{2}[A][B'_G]\{d\} \tag{8}$$

where, $[B'_0]$ and $[B'_{nl}]$ are strain-displacement matrices with respect to linear and nonlinear strain components respectively in local co-ordinate system (x' - y' - z'). The normal strain ε_z' along z' direction is neglected.

Knowing, the stress-strain relationship of the laminated composite material in each layer in its material axis system (1 - 2 - 3), the stress-strain relationship in the local co-ordinate systems (x' - y' - z') can be found out by simple transformation. Here material axis *3* is directed along z' direction. The material axes 1 - 2 lie in x' - y' plane but it can be oriented at some angle θ. After transforma- tion the stress-strain relationship in the local co-ordinate systems can be written as

$$\{\sigma'\} = [D]\{\varepsilon'\} \tag{9}$$

After finding $[B'_0]$, $[B'_{nl}]$ and $[D']$ matrices the secant stiffness matrix can be expressed as

$$[k]_S = \int [B'_0]^T [D'][B'_0]dV + \frac{1}{2}\int [B'_0]^T [D'][B'_{nl}]dV + \int [B'_{nl}]^T [D'][B'_0]dV + \frac{1}{2}[B'_{nl}]^T [D'][B'_{nl}]dV \tag{10}$$

This secant stiffness matrix is not symmetric. To efficiently use the storage scheme which is used in linear analysis, this non symmetric scant stiffness matrix can be made symmetric (Wood and Schrefler 1978) as

$$\begin{aligned}[k]_S = &\int [B'_0]^T [D'][B'_0]dV + \frac{1}{2}\int [B'_0]^T [D'][B'_{nl}]dV + \frac{1}{2}\int [B'_{nl}]^T [D'][B'_0]dV \\ &+ \frac{1}{3}\int [B'_{nl}]^T [D'][B'_{nl}]dV + \frac{1}{2}\int [B'_G]^T [\tau][B'_G]dV + \frac{1}{3}\int [B'_G]^T [\tau_{nl}][B'_G]dV\end{aligned} \tag{11}$$

where, $[D']$ matrix is stress-strain matrix in local co-ordinate system, and $[\tau]$ and $[\tau_{nl}]$ are stress matrix in local co-ordinate system for linear and nonlinear parts of the strain respectively.

The tangent stiffness matrix, which is used in the nonlinear solution of the equilibrium equation by Newton-Raphson method, can be written as

$$\begin{aligned}[k]_T = &\int [B'_0]^T [D'][B'_0]dV + \int [B'_0]^T [D'][B'_{nl}]dV + \int [B'_{nl}]^T [D'][B'_0]dV \\ &+ \int [B'_{nl}]^T [D'][B'_{nl}]dV + \frac{1}{2}\int [B'_G]^T [\tau + \tau_{nl}][B'_G]dV\end{aligned} \tag{12}$$

2.2 Stiffener element

The derivation of the stiffener element (Fig. 2) is based on the basic concept used to derive the shell element. In this case the stiffener element modeled with three dimensional solid element is degenerated with the help of certain extractions obtained from the consideration that the dimension across stiffener depth as well as breadth is small compared to that along the length.

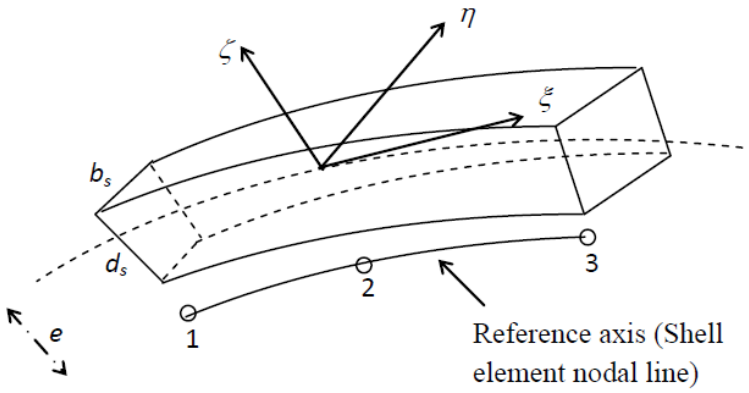

Fig. 2 Degenerated curved beam element

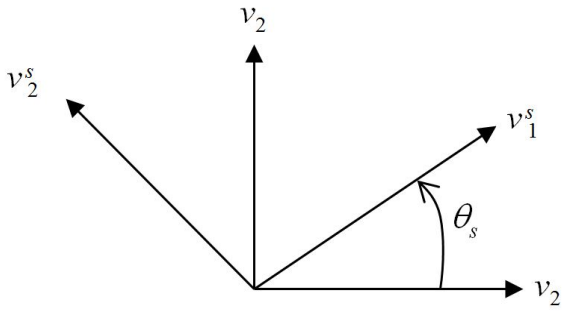

Fig. 3 Orientation of stiffener local axis with respect to shell local axis (Plan view)

The stiffener element follows an edge of a shell element where the parameters of three nodes lying on that shell element edge are used to express the geometry and deformation of the stiffener utilizing compatibility between shell and stiffeners. It helps to eliminate the involvement of additional degrees of freedom for the modeling of stiffeners. The stiffener element having any arbitrary curved geometry is mapped into a regular domain in ξ - η - ζ co-ordinate system where all these coordinates vary from -1 to $+1$. Again ξ is taken along the stiffener axis while η and ζ are taken along the width and depth directions respectively. It has been found that the vectors v_{1i}, v_{2i} and v_{3i} of the shell element are quite useful for the representation of geometry and deformation of the stiffener element. For the stiffener element a similar set of vectors v_{1i}^s, v_{2i}^s and v_{3i}^s are used and these may be obtained from those of the shell element (v_{1i}, v_{2i} and v_{3i}) as

$$v_1^s = v_1 \cos\theta_s + v_2 \sin\theta_s, \quad v_2^s = -v_1 \sin\theta_s + v_2 \cos\theta_s \quad \text{and} \quad v_3^s = v_3 \tag{13}$$

where (v_{1i}^s - v_{2i}^s) is oriented at an angle of θ_s with respect to (v_{1i} - v_{2i}) and v_{1i}^s follows the stiffener axis (Fig. 3).

The direction of the vectors v_{1i}^s, v_{2i}^s and v_{3i}^s are the direction of the local co-ordinate system x', y' and z' directions respectively for the stiffeners, which are used in the stiffener element's stain-deformation and stress-strain relationships. The component of these vector are direction

cosines of x', y' and z' lines with respect to the global (x - y - z) co-ordinate. l^s_{1i}, m^s_{1i} and n^s_{1i} aredirection cosine of x' axis for stiffener, those are same as the component of unit vector v^s_{1i}, l^s_{2i}, m^s_{2i} and n^s_{2i} are direction cosine of y' axis for stiffener, those are same as the component of unit vector v^s_{2i} and l^s_{3i}, m^s_{3i} and n^s_{3i} are direction cosine of z' axis for stiffener, those are same as the component of unit vector v^s_{3i}.

With these vectors, the co-ordinates of any point within the stiffener may be expressed in terms of co-ordinates (x_i, y_i, z_i) of those three nodes of the corresponding shell element edge as

$$\begin{Bmatrix} x \\ y \\ z \end{Bmatrix} = \sum_{i=1}^{3} N_{si}(\xi) \begin{Bmatrix} x_i \\ y_i \\ z_i \end{Bmatrix} + \sum_{i=1}^{3} N_{si}(\xi) \left(\frac{\zeta \times d_s}{2} + e \right) \begin{Bmatrix} l_{3i} \\ m_{3i} \\ n_{3i} \end{Bmatrix} + \sum_{i=1}^{3} N_{si}(\xi) \left(\frac{\eta \times b_s}{2} \right) \begin{Bmatrix} l^s_{2i} \\ m^s_{2i} \\ n^s_{2i} \end{Bmatrix} \tag{14}$$

where b_s is stiffener width, d_s is its depth and e is the eccentricity (distance of the stiffener axis from the shell mid surface, taken positive when the stiffener is attached to the top of the plate and taken negative when the stiffener is attached to the bottom), N_{si} are the expressions of the quadratic shape functions along ξ-direction $\left(N_{s1} = \frac{\xi(\xi-1)}{2},\ \ N_{s2} = 1-\xi^2,\ \ N_{s3} = \frac{\xi(\xi+1)}{2} \right)$.

Now considering the deformation of the stiffener element, the present formulation differs from the usual one (Bathe 1996, Ferguson and Clark 1979, Liao and Reddy 1990) where six degrees of freedom are generally taken to represent the biaxial bending apart from torsion and axial deformation. In the present study the bending of the stiffener in the tangential plane of the shell is not considered. This has helped to eliminate the involvement the sixth degrees of freedom θ_z like that of shell element. Moreover the usual formulation (Bathe 1996, Ferguson and Clark 1979, Liao and Reddy 1990) overestimates the torsional rigidity and it cannot be corrected simply with some correction factor since it got mixed with other terms. In these cases the warping displacement in the stiffener element is also neglected. However, the present formulation facilitates to treat it nicely where a torsion correction factor is introduced for parallel as well as perpendicular stacking schemes (Figs. 4(a) and (b)). Actually this is the primary object for the reformulation of the stiffener element. Based on this the displacement components at any point within the stiffener may be expressed as

$$\begin{Bmatrix} u \\ v \\ w \end{Bmatrix} = \sum_{i=1}^{3} N_{si}(\xi)[T_{vi}] \begin{Bmatrix} u_i \\ v_i \\ w_i \end{Bmatrix} - \sum_{i=1}^{3} N_{si}(\xi) \left(\frac{\zeta \times d_s}{2} + e \right) \begin{bmatrix} l^s_{1i} & l^s_{2i} \\ m^s_{1i} & m^s_{2i} \\ n^s_{1i} & n^s_{2i} \end{bmatrix} \begin{Bmatrix} \theta^s_{xi} \\ \theta^s_{yi} \end{Bmatrix} = [N_{Ds}]\{\delta_s\} \tag{15}$$

where, θ^s_{xi} and θ^s_{yi} are rotations about local y' and x' axes (i.e., v^s_{2i} and v^s_{1i}) of the stiffener node respectively. θ^s_{xi} and θ^s_{yi} can be written as

$$\theta^s_{xi} = \cos\theta_s \times \theta_x + \sin\theta_s \times \theta_y \quad \text{and} \quad \theta^s_{yi} = -\sin\theta_s \times \theta_x + \cos\theta_s \times \theta_y \tag{16}$$

Using Eq. (16) in Eq. (15), the displacement components at any point within the stiffener can be expressed with the help of unit vectors and rotations at shell mid surface node as

$$\begin{Bmatrix} u \\ v \\ w \end{Bmatrix} = \sum_{i=1}^{3} N_{si}(\xi)[T_{vi}] \begin{Bmatrix} u_i \\ v_i \\ w_i \end{Bmatrix} - \sum_{i=1}^{3} N_{si}(\xi) \left(\frac{\zeta \times d_s}{2} + e \right) \begin{bmatrix} l_{1i} & l_{2i}^s \\ m_{1i} & m_{2i}^s \\ n_{1i} & n_{2i}^s \end{bmatrix} \begin{Bmatrix} \theta_{xi} \\ \theta_{yi} \end{Bmatrix} = [N_{Ds}]\{\delta_s\} \tag{17}$$

where, $\{\delta_s\}$ is the displacement vector of stiffener element, which is same as the displacement vector of the three nodes of the shell element coming in line with the stiffener element, $\{\delta_s\} = [u_1\ v_1\ w_1\ \theta_{x1}\ \theta_{y1}\ u_2\ u_2 - - - - \theta_{y3}]^T$.

The matrix $[T_{vi}]$ is used to make the component of translational displacement along v_{2i}^s at shell mid-plane as zero, since the bending of the stiffener in the tangential plane of the shell is not considered. Its effect should be insignificant since bending deformation in this mode will be very small due to high in-plane rigidity of the shell skin. This assumption will not affect the accuracy of the solution. Moreover the flexural rigidity of stiffener in this mode is usually found to be small.

The matrix $[T_{vi}]$ used in the above equation may be expressed with the help of v_{1i}^s, v_{2i}^s as

$$[T_{vi}] = \begin{bmatrix} l_{1i}^s & l_{2i}^s & l_{3i}^s \\ m_{1i}^s & m_{2i}^s & m_{3i}^s \\ n_{1i}^s & n_{2i}^s & n_{3i}^s \end{bmatrix} \begin{bmatrix} l_{1i}^s & m_{1i}^s & n_{1i}^s \\ 0 & 0 & 0 \\ l_{3i}^s & m_{3i}^s & n_{3i}^s \end{bmatrix} \tag{18}$$

The strain displacement relationship with Green-Lagrange strain of the stiffener element in local co-ordinate system (x' - y' - z') of the stiffener can be expressed as

$$\{\varepsilon'\} = \begin{Bmatrix} \varepsilon_x' \\ \gamma_{x'z'} \\ \gamma_{x'y'} \end{Bmatrix} = \begin{Bmatrix} \dfrac{\partial u'}{\partial x'} \\ \dfrac{\partial u'}{\partial z'} + \dfrac{\partial w'}{\partial x'} \\ \dfrac{\partial u'}{\partial y'} + \dfrac{\partial v'}{\partial x'} \end{Bmatrix} + \begin{Bmatrix} \dfrac{1}{2}\left(\left(\dfrac{\partial u'}{\partial x'} \right)^2 + \left(\dfrac{\partial v'}{\partial x'} \right)^2 + \left(\dfrac{\partial w'}{\partial x'} \right)^2 \right) \\ \left(\dfrac{\partial u'}{\partial x'} \times \dfrac{\partial u'}{\partial y'} + \dfrac{\partial v'}{\partial x'} \times \dfrac{\partial v'}{\partial z'} + \dfrac{\partial w'}{\partial x'} \times \dfrac{\partial w'}{\partial z'} \right) \\ \left(\dfrac{\partial u'}{\partial x'} \times \dfrac{\partial u'}{\partial y'} + \dfrac{\partial v'}{\partial x'} \times \dfrac{\partial v'}{\partial y'} + \dfrac{\partial w'}{\partial x'} \times \dfrac{\partial w'}{\partial y'} \right) \end{Bmatrix} \tag{19}$$

$$\{\varepsilon'\} = [B_{0s}']\{\delta_s\} + \frac{1}{2}[B_{nls}']\{\delta_s\} \tag{20}$$

$$\{\varepsilon'\} = [B_{0s}']\{\delta_s\} + \frac{1}{2}[A_s][B_{Gs}']\{\delta_s\} \tag{21}$$

The strains $\varepsilon_{y'}$ and $\gamma_{y'z'}$ are neglected in the stiffener element.

Similar to the shell element, the stress and strain components at any point within the stiffener element are taken in a local axis system (x' - y' - z') corresponding to v_{1i}^s, v_{2i}^s and v_{3i}^s. The relationship between them may be expressed as

$$\begin{Bmatrix} \sigma' \\ \tau_{x'z'} \\ \tau_{x'y'} \end{Bmatrix} = \begin{bmatrix} \overline{Q}_{1m} & 0 & 0 \\ 0 & \beta_s \overline{Q}_{5m} & 0 \\ 0 & 0 & \beta_t \overline{Q}_{6m} \end{bmatrix} \begin{Bmatrix} \varepsilon_{x'} \\ \gamma_{x'z'} \\ \gamma_{x'y'} \end{Bmatrix} \quad \text{or} \quad \{\sigma'\} = [D_s']\{\varepsilon'\} \tag{22}$$

where β_s is the shear correction factor, which is taken as 5/6. The torsion correction factor β_t and other rigidity parameters in the rigidity matrix $[D'_s]$ in Eq. (22) are presented for two different types of stacking arrangements of the stiffener as shown in Fig. 4(a) (parallel stacking) and Fig. 4(b) (perpendicular stacking). For both the arrangements, the fibers are oriented with respect to x' axis. The material axis system is 1 - 2 - 3. Axes 1 - 2 is oriented with x' - r by angle θ, while direction 3 is along the direction of s. In both the arrangements, the stress-strain relationship of a lamina in its axis system (x' - r - s) as shown in Figs. 4(a) and (b), after transforming from their material axis system (1 - 2 - 3) can be written as

$$\begin{Bmatrix} \sigma' \\ \sigma_r \\ \tau_{x'r} \\ \tau_{x's} \\ \tau_{rs} \end{Bmatrix} = \begin{bmatrix} \overline{Q}_{11} & \overline{Q}_{12} & \overline{Q}_{16} & 0 & 0 \\ \overline{Q}_{21} & \overline{Q}_{22} & \overline{Q}_{26} & 0 & 0 \\ \overline{Q}_{61} & \overline{Q}_{62} & \overline{Q}_{66} & 0 & 0 \\ 0 & 0 & 0 & \overline{Q}_{55} & \overline{Q}_{54} \\ 0 & 0 & 0 & \overline{Q}_{45} & \overline{Q}_{44} \end{bmatrix} \begin{Bmatrix} \varepsilon_{x'} \\ \varepsilon_r \\ \gamma_{x'r} \\ \gamma_{x's} \\ \gamma_{rs} \end{Bmatrix} \tag{23}$$

In (x' - r - s) axes system for Ply arrangement-I, r corresponds to y' and s corresponds to z', while in Ply arrangement-II, s corresponds to negative y' and r corresponds to z', of the local axis system (x' - y' - z'). The orientation of x' of (x' - r - s) axis system is same as the orientation of x' of (x' - y' - z') in both cases of arrangement. So the rigidity parameters $[D'_s]$ in Eq. (22) is found out separately for both arrangements of ply with respect to (x' - r - s) axes system. The local axes are required to be found out in each node and integration point to evaluate the strain-displacement matrices. In a particular layer $[D'_s]$ remains constant. It will change from layer to layer. Even if two layers have same ply orientation, the torsion correction factor β_t changes from layer to layer.

The rigidity parameters $[D'_s]$ of Eq. (22) may be obtained by modifying the Eq. (23), utilizing the conditions ($\sigma_r = 0$) and ($\tau_{rs} = 0$).

For ply arrangement-I, the rigidity parameters will be

$$\overline{Q}_{1m} = \overline{Q}_{11} + \overline{Q}_{12}\frac{\overline{Q}_{61}\overline{Q}_{21} - \overline{Q}_{21}\overline{Q}_{66}}{\overline{Q}_{22}\overline{Q}_{66} - \overline{Q}_{62}\overline{Q}_{26}} + \overline{Q}_{16}\frac{\overline{Q}_{61}\overline{Q}_{22} - \overline{Q}_{21}\overline{Q}_{62}}{\overline{Q}_{26}\overline{Q}_{62} - \overline{Q}_{66}\overline{Q}_{22}} \tag{24}$$

$$\overline{Q}_{5m} = \overline{Q}_{55} - \overline{Q}_{54}\frac{\overline{Q}_{45}}{\overline{Q}_{44}} \tag{25}$$

$$\overline{Q}_{6m} = \overline{Q}_{66} \tag{26}$$

$$\beta_t = \frac{3kb_s^2\sum_{i=1}^{nls}\overline{Q}_{5m}^i(s_{i+1} - s_i)}{\sum_{i=1}^{nls}\overline{Q}_{6m}^i(s_{i+1}^3 - s_i^3)} \tag{27}$$

For ply arrangement-II, the rigidity parameters will be

$$\overline{Q}_{1m} = \overline{Q}_{11} + \overline{Q}_{12}\frac{\overline{Q}_{61}\overline{Q}_{21} - \overline{Q}_{21}\overline{Q}_{66}}{\overline{Q}_{22}\overline{Q}_{66} - \overline{Q}_{62}\overline{Q}_{26}} + \overline{Q}_{16}\frac{\overline{Q}_{61}\overline{Q}_{22} - \overline{Q}_{21}\overline{Q}_{62}}{\overline{Q}_{26}\overline{Q}_{62} - \overline{Q}_{66}\overline{Q}_{22}} \tag{28}$$

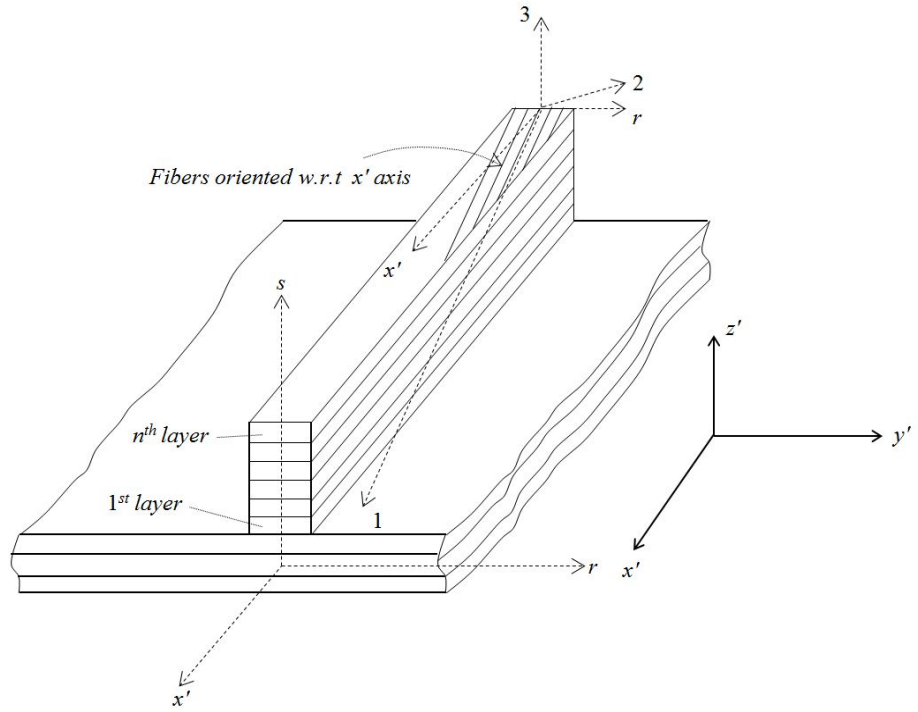

(a)

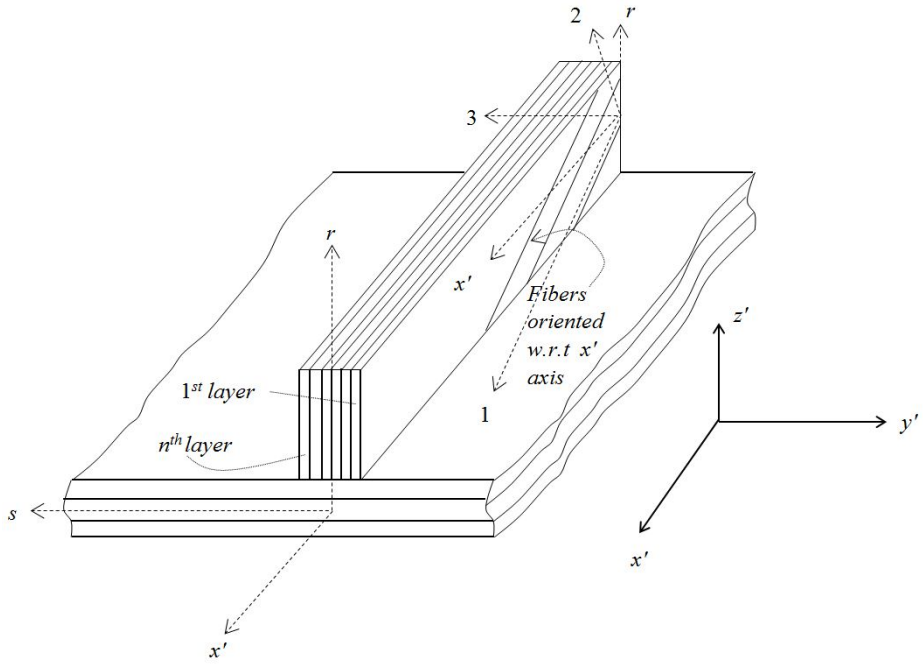

(b)

Fig. 4 (a) Ply arrangement-I in stiffener (Parallel stacking); (b) Ply arrangement-II in stiffener (Perpendicular stacking)

$$\overline{Q}_{5m} = \overline{Q}_{66} \tag{29}$$

$$\overline{Q}_{6m} = \overline{Q}_{55} - \overline{Q}_{54}\frac{\overline{Q}_{45}}{\overline{Q}_{44}} \tag{30}$$

$$\beta_t = \frac{12kd_s\sum_{i=1}^{nls}\overline{Q}_{5m}^{i}(s_{i+1}^3 - s_i^3)}{\left[\left(d_s + \frac{h}{2}\right)^3 - \left(\frac{h}{2}\right)^3\right]\sum_{i=1}^{nls}\overline{Q}_{6m}^{i}(s_{i+1} - s_i)} \tag{31}$$

where *nls* is the number of layers of the stiffener rib and *k* is the factor to get torsion constant of an isotropic beam having rectangular section, which is a function of d_s/b_s ratio of the rectangular section (Timoshenko and Goodier 1951).

After finding $[B'_{0s}]$, $[B'_{nls}]$ and $[D'_s]$ matrices, the secant and tangent stiffness matrices of the stiffener element can be obtained by following the same procedure as done in the shell element.

The secant and tangent stiffness matrices of all elements of the plate and stiffeners are calculated and assembled properly to form the global secant and tangent stiffness matrices of the structure. The load vector is calculated. The nonlinear equations are solved by the Newton-Raphson iteration technique along with the incremental method using Cholesky decomposition method. The tolerance is defined with respect to the residual load.

2.3 Nodal load vector

The element load vector due to externally applied distributed load can be derived in a similar manner with the help of Eq. (3) and it may be expressed as

$$[f_e] = \int [N_D]^T \begin{Bmatrix} q_x \\ q_y \\ q_z \end{Bmatrix} |J|\, d\xi\, d\eta\, d\zeta \tag{32}$$

where q_x, q_y and q_z are the components of the intensity of the distributed load per unit volume along x, y and z, respectively. If the distributed load acts on the top surface ($\zeta = +1$) or bottom surface ($\zeta = -1$), the quantity in Eq. (32) will be computed for the specific value of ζ while the integration will be carried out only in the ($\xi - \eta$) plane. In that case, intensity of the distributed load will be defined as load per unit area.

2.4 Solution of equations

For an elastic continuum undergoing small or large deformation, the equilibrium of external and internal forces can be expressed by virtual work equation as

$$\{\psi\}d\{\Delta\}^T = \int d\{\varepsilon\}^T\{\sigma\}dv - \{F\}d\{\Delta\}^T = \{0\} \tag{33}$$

where

$\{\Delta\}$ = Nodal displacements of the discretized continuum,
$\{\psi\}$ = Resultant of external and internal forces,
$\{\sigma\}$ = Stress
$\{\varepsilon\}$ = Strain
$\{F\}$= Applied load

Again

$$d\{\varepsilon\} = [B]d\{\Delta\}, \quad \text{and} \quad [B] = [B_0] + [B_{nl}] \tag{34}$$

$$d\{\varepsilon\} = \left[[B_0] + [B_{nl}]\right]d\{\Delta\} \tag{35}$$

$$d\{\varepsilon\}^T = d\{\Delta\}^T\left[[B_0] + [B_{nl}]\right]^T \tag{36}$$

Also, we can write

$$\{\sigma\} = [D]\{\varepsilon\} \tag{37}$$

$$\{\varepsilon\} = [B_0]\{\Delta\} + \frac{1}{2}[B_{nl}]\{\Delta\}, \quad \text{or} \quad \{\varepsilon\} = \left[[B_0] + \frac{1}{2}[B_{nl}]\right]\{\Delta\} \tag{38}$$

$$\{\sigma\} = [D]\left[[B_0] + \frac{1}{2}[B_{nl}]\right]\{\Delta\} \tag{39}$$

Now, using Eqs. (36) and (39) in Eq. (33), we can write

$$\{\psi\}d\{\Delta\}^T = \int d\{\Delta\}^T\left[[B_0] + [B_{nl}]\right]^T[D]\left[[B_0] + \frac{1}{2}[B_{nl}]\right]\{\Delta\}dv - \{F\}d\{\Delta\}^T = \{0\} \tag{40}$$

Eliminating, $d\{\Delta\}^T$ form both sides the Eq. (40) becomes

$$\{\psi\} = \left[\int\left[[B_0] + [B_{nl}]\right]^T[D]\left[[B_0] + \frac{1}{2}[B_{nl}]\right]dv\right]\{\Delta\} - \{F\} = \{0\} \tag{41}$$

Or

$$\{\psi\} = [K_s]\{\Delta\} - \{F\} = \{0\} \tag{42}$$

and

$$[K_s] = \int\left[[B_0] + [B_{nl}]\right]^T[D]\left[[B_0] + \frac{1}{2}[B_{nl}]\right]dv \tag{43}$$

where, $[K_s]$ = secant stiffness matrix, which is similar to the matrix in Eq. (10).

Eq. (42) is the final equilibrium matrix either in elemental level or in global level, which is to be solved. Eq. (33) to Eq. (43) are the equations written in general sense, i.e., without any specific

axis system. So we can evaluate all the parameters in these equations in our required axis system and we can solve the Eq. (42) either in elemental level or in global level.

In the present case the all the parameters are evaluated in the local axis system and the equilibrium equation is solved in a global (assembled) sense. The Eq. (42) is a nonlinear equation as it contains the nonlinear terms of the square of derivatives of the displacements. The derivatives of the displacements are strains. In this case the nonlinear equilibrium Eq. (42) is solved by Newton-Raphson iteration technique along with the incremental method. First different load steps are selected and in each load step the Newton-Raphson iteration technique is followed to get the conversed solution in that step. The solution in the n^{th} load step is used in the solution in n + 1th load step. In a particular load step as the solution converges the difference between the external load and the internal force developed tends to zero, i.e., $\{\psi\}$ tends to zero. The iterations should go up to the point where $\{\psi\}$ attains zero value, for this a tolerance is specified. In each iteration the load deformation (equilibrium) equation is solved by Cholesky decomposition method.

In order to solve the nonlinear equilibrium equation by Newton-Raphson, we have to follow the following steps. Suppose, at ith iteration the solution of deformations is $\{\Delta\}^i$, and at this deformation the resultant of external and internal forces(also called as unbalanced forces) is $\{\psi\}^i$. Then in the next iteration at $i+1$, an improved solution of value $\{\Delta\}^{i+1}$ can be obtained by a Taylor series expansion (with one term) of $\{\psi\}^i$ (i.e., in its neighbour point) as

$$\{\psi\}^{i+1} = \{\psi\}^i + \frac{d\{\psi\}^i}{d\{\Delta\}^i}\{\delta\Delta\}^i = \{0\} \tag{44}$$

$$\{\Delta\}^{i+1} = \{\Delta\}^i + \{\delta\Delta\}^i \tag{45}$$

$\frac{d\{\psi\}^i}{d\{\Delta\}^i} = [K_T]^i$, called as tangent stiffness matrix, it can be evaluated from the incremental equilibrium equation. The value obtained is similar to the Eq. (12).

Now, we can write

$$\{\psi\}^i + [K_T]^i\{\delta\Delta\}^i = \{0\} \tag{46}$$

Putting the value of $\{\psi\}^i$ from Eq. (42) in Eq. (46), we get

$$[K_s]^i\{\Delta\}^i - \{F\} + [K_T]^i\{\delta\Delta\}^i = \{0\} \tag{47}$$

Or

$$[K_T]^i\{\delta\Delta\}^i = \{F\} - [K_s]^i\{\Delta\}^i \quad \text{or} \quad \{\delta\Delta\}^i = \left[[K_T]^i\right]^{-1}\left\{\{F\} - [K_s]^i\{\Delta\}^i\right\} \tag{48}$$

After finding $\{\delta\Delta\}^i$, we can find

$$\{\Delta\}^{i+1} = \{\Delta\}^i + \{\delta\Delta\}^i \tag{49}$$

In the first load step, initially a linear equilibrium is solved to get $\{\Delta\}$ for the load of that step. Once this is obtained we proceed for the nonlinear solution. In the first iteration of the nonlinear

solution the $\{\delta\Delta\}^1$ is obtained. Then the total deformation in the first iteration becomes summation of linear solution plus the $\{\delta\Delta\}^1$. In the second iteration we calculate $\{\delta\Delta\}^2$ and final deformation in this iteration is total of first iteration plus $\{\delta\Delta\}^2$. Similarly we proceed till the results are converged. For the convergence we can use different criterion. In the present method the convergence of load is adopted. The iteration process terminates when

$$\frac{\left\{\{\psi\}^T\{\psi\}\right\}^{\frac{1}{2}}}{\left\{\{F\}^T\{F\}\right\}^{\frac{1}{2}}}\times 100 \le \text{Tolerance} \tag{50}$$

In the present analysis 1% Tolerance has been adopted for all the analysis carried out.

3. Results

The convergence and validation of the present formulation is tested considering the systems solved by previous researchers. The definition of the problem for the present analysis is presented. The numerical results and the parametric study of the present system is reported. The formulation and the analysis are done by writing a computer program in FORTRAN 90.

3.1 Convergence and validation

The convergence and validation of the present formulation is tested first. Then the results of the present problem under investigation are presented.

3.1.1 Two bay rectangular isotropic stiffened plate

An isotropic stiffened plate (1000 mm × 500 mm × 3 mm) with a central stiffener (depth = 18 mm, breadth = 10 mm) along the shorter direction, clamped on all sides is considered for the convergence study and validation purpose of the present formulation. The Young's modulus of the plate is 71700 N/mm^2 and Poission's ratio is 0.33. The central deflection of the plate with different mesh size for two loading intensity is presented in Table 1. It is seen from the table that the results are converging quickly with the increase in the mesh size. The 8 × 8 mesh size of the full plate is sufficient to get the converged result.

The result of this problem with 8 × 8 mesh of full plate is compared with the results of Sheikh

Table 1 Central deflection of the isotropic stiffened plate

Mesh size (full plate)	Central deflection in mm	
	Load intensity (0.1 N/mm^2)	Load intensity (1.0 N/mm^2)
2 × 2	4.766	23.480
4 × 4	3.418	16.251
6 × 6	3.284	15.426
8 × 8	3.268	15.272
10 × 10	3.258	15.307

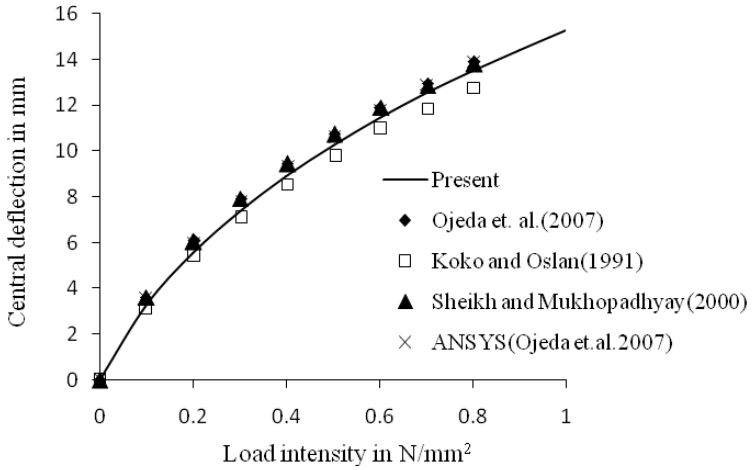

Fig. 5 Central deflection of isotropic stiffened plate

and Mukhopadhyay (2000) by spline finite strip method, Ojeda *et al*. (2007) by finite element method, Koko and Oslan (1991) by super element method as well as by semi-analytic finite strip method and ANSYS solved by Ojeda *et al*. (2007) in Fig. 5, to further validate the formulation. Sheikh and Mukhopadhyay (2000) and Ojeda *et al*. (2007) have used the Green-Lagrange strain-displacement relationship with von Karman's assumption. However, in the present formulation, full Green-Lagrange strain-displacement relationship is used. It is seen from Fig. 5 that the results obtained in the present formulation are matching well with others' results.

3.1.2 Cross-stiffened laminated composite stiffened plate

A simply supported cross stiffened composite square plate (2438 mm × 2438 mm × 6.35 mm) as shown in Fig. 6 is taken to further validate the formulation. This plate has been analyzed for cross-ply (0 / 90) and angle-ply (– 45 / 45) lamination schemes. The stiffeners are attached on both sides of the plate on both x and y directions as shown in the Fig. 6. The lamination scheme in the plates and stiffeners are same. The stiffener depth, d_s = 6.35 mm and breadth, b_s = 20 mm. The material properties of the plate as well as stiffeners are $E_1 = 25E_2$, E_2 = 7031 N/mm^2, $G_{12} = G_{13} = 0.5E_2$, $G_{23} = 0.2E_2$ and $\nu_{12} = 0.25$. Two types of simply supported boundary conditions, BC-1 and BC-2 are considered.

BC-1,

Side-1 and Side-2, $u = w = \varphi_x = 0$ (φ_x is the rotation about y-axis)
Side-3 and Side-4, $v = w = \varphi_y = 0$ (φ_y is the rotation about x-axis)

BC-2,

Side-1 and Side-2, $v = w = \varphi_x = 0$ (φ_x is the rotation about y-axis)
Side-3 and Side-4, $u = w = \varphi_y = 0$ (φ_y is the rotation about x-axis)

The central deflection of the plate with BC-1 for different mesh size for two loading intensity for both, cross-ply and angle-ply lamination schemes are presented in Table 2. In this case also

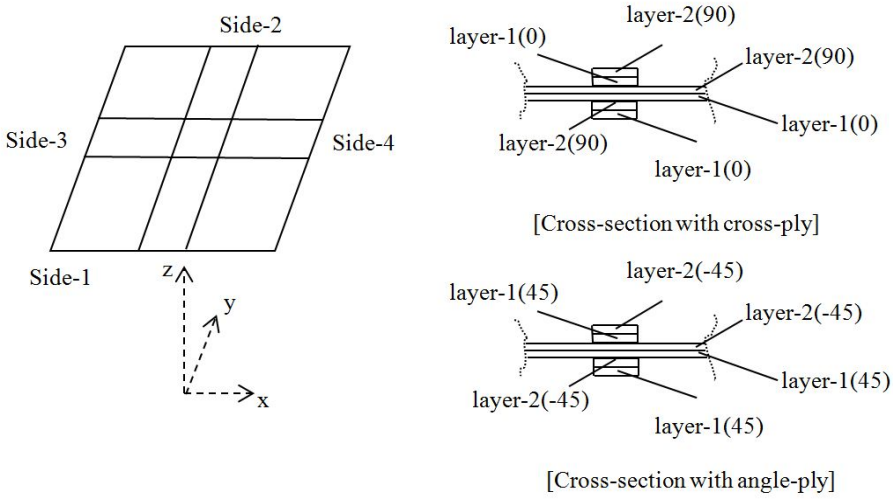

Fig. 6 Crossed-stiffened plate with cross-section at stiffener with two layers

the results are converging quickly with the increase in the mesh size. The 8 × 8 mesh size of the full plate is sufficient to get the converged result. So in the present analysis 8 × 8 mesh of the full plate is adopted.

Again to validate the formulation further, the central deflection of the plate with BC-1 are presented in Figs. 7(a) and (b) for angle-ply and cross-ply lamination scheme respectively along with the results obtained from ABAQUS finite element software. The stiffeners are modeled with shell element in ABAQUS and the required shells are tied up with tie constraint (surface-surface). The element used in the ABAQUS model is S8R5. The results are matching well.

Results for this example with BC-2 have been previously reported by Chattopadhyay *et al*. (1995), Liao and Reddy (1990) and Ojeda *et al*. (2007). The result of this problem with BC-2 for angle-ply lamination and cross-ply lamination scheme is compared with the finite element results of Chattopadhyay *et al*. (1995), Liao and Reddy (1990) and Ojeda *et al*. (2007) along with the results obtained from ABAQUS software, in Figs. 8(a) and (b), respectively. The results are matching well.

Table 2 Central deflection of the laminated composite crossed-stiffened plate (with BC-1)

Mesh size (full plate)	Central deflection in mm			
	Cross-ply scheme		Angle-ply scheme	
	Load intensity (2.0×10^{-5} N/mm^2)	Load intensity (1.0×10^{-4} N/mm^2)	Load intensity (2.0×10^{-5} N/mm^2)	Load intensity (1.0×10^{-4} N/mm^2)
2 × 2	1.050	5.028	1.710	5.751
4 × 4	3.655	11.569	2.145	6.486
6 × 6	3.825	11.780	2.277	6.563
8 × 8	3.839	11.869	2.296	6.652

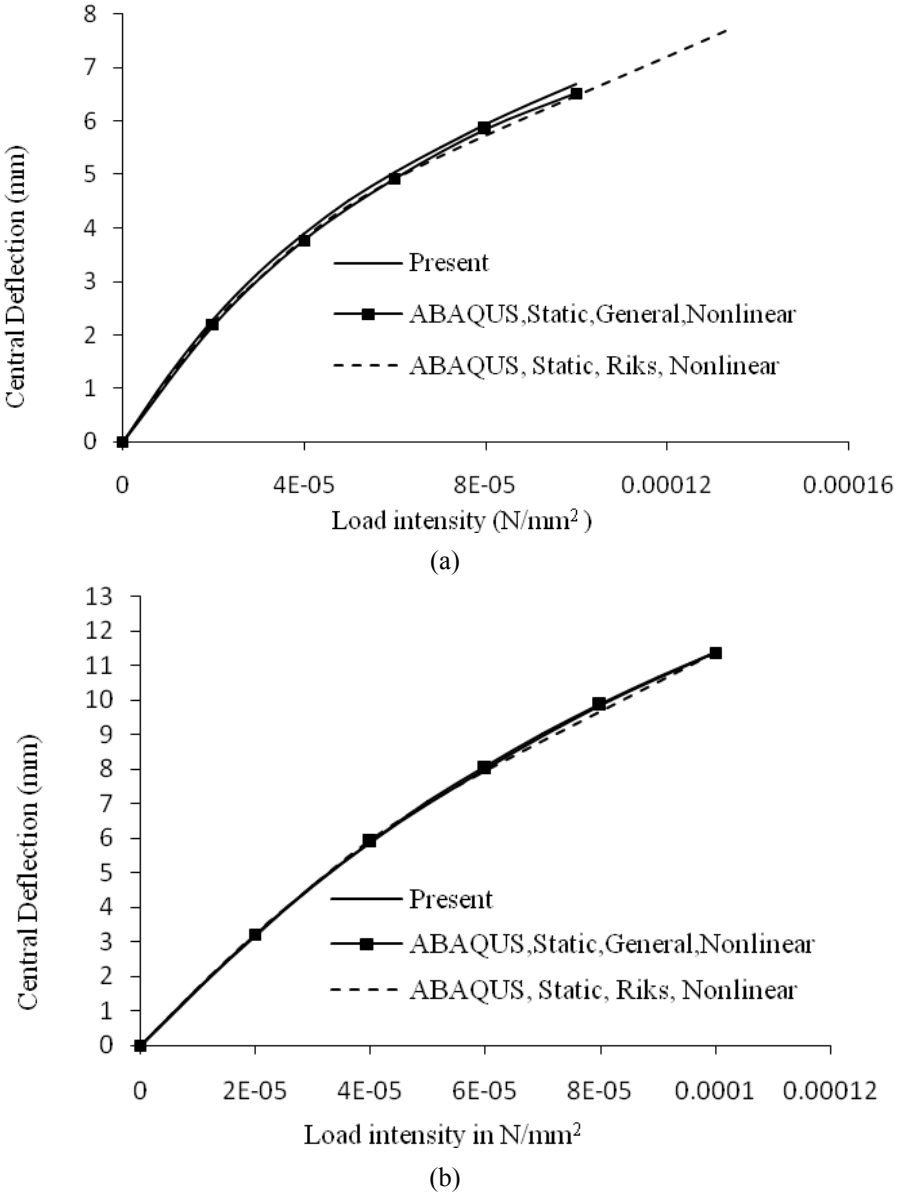

Fig. 7 (a) Central deflection of the crossed-stiffened plate with (–45/45) lamination (BC-1); (b) Central deflection of the crossed-stiffened plate with (0/90) lamination scheme (BC-1)

3.2 Problem under investigation

The basic configuration of the problem considered here (Fig. 9) is a square laminated composite stiffened plate (1000 mm × 1000 mm × 10 mm) with a central x-directional stiffener (d_s (depth) = 20 mm and b_s (breadth) = 10 mm) subjected to uniformly distributed transverse loading. The lamination scheme adopted is $(\theta/-\theta)_n$ for plate and stiffener, n varies from 1 to 4. The

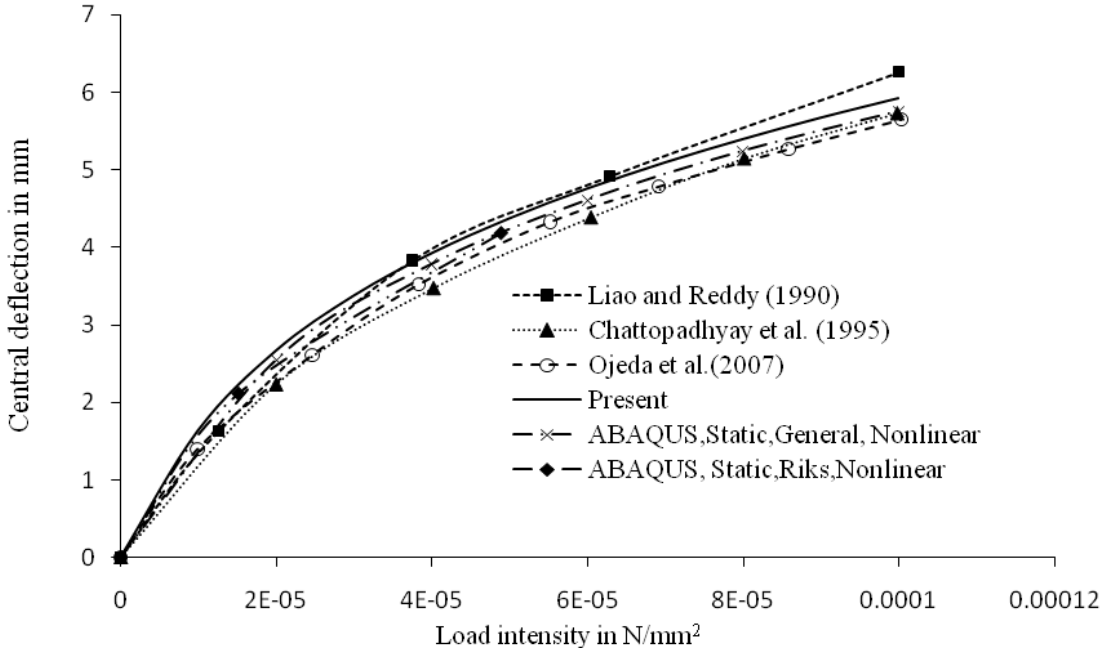

(a)

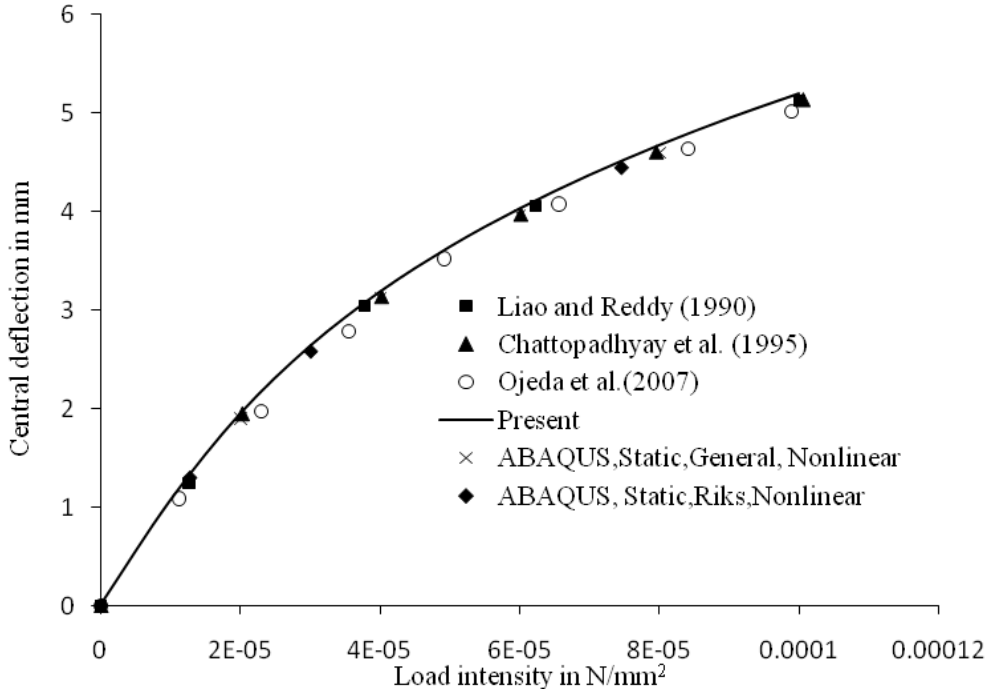

(b)

Fig. 8 (a) Central deflection of the crossed-stiffened plate with (–45 / 45) lamination (BC-2); (b) Central deflection of the crossed-stiffened plate with (0 / 90) lamination scheme (BC-2)

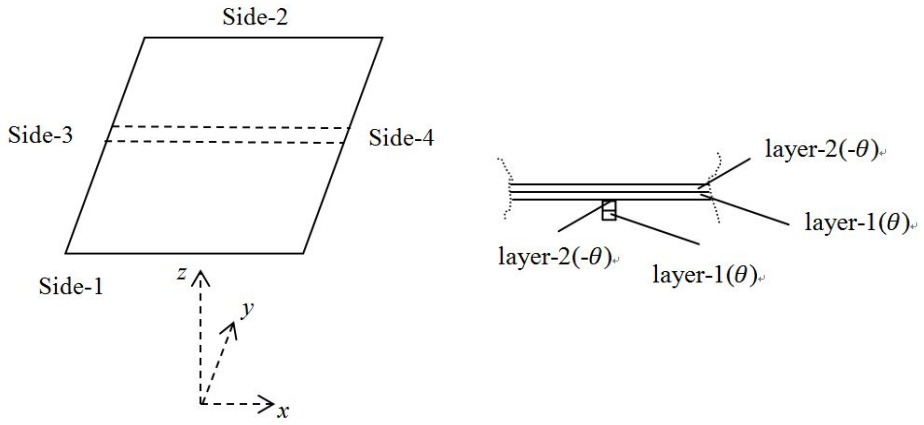

Fig. 9 Stiffened plate with cross-section at stiffener with two layers of lamina

numbering of layers starts from bottom to top in plate as well as in stiffeners. The stiffeners are attached at the bottom of the plate. All four sides are simply supported.

Simply supported boundary condition:

Side-1 and Side-2, $u = w = \varphi_x = 0$ (φ_x is the rotation about y-axis)
Side-3 and Side-4, $v = w = \varphi_y = 0$ (φ_y is the rotation about x-axis)

3.3 Numerical results of the present problem

The numerical results of the considered system are presented in this section considering different parameters.

3.3.1 Effect of lamination angle

The central deflection of the simply supported laminated composite stiffened plate considering 8×8 mesh of the whole plate is computed for two layers $(\theta/-\theta)_1$ plate and stiffener, taking θ form 0° to 90° with the interval of 15°. The material properties of the plate as well as stiffener are, $E_1 = 25E_2$, $E_2 = 7031$ N/mm^2, $G_{12} = G_{13} = 0.5E_2$, $G_{23} = 0.2E_2$, $v_{12} = 0.25$ and d_s (depth of stiffener) = 20 mm. The stacking in the stiffener is horizontal. The results are presented in Fig. 10.

It is observed that the stiffened plate with $(45/-45)$ skin and s stiffer among all lamination angle and plate with $(90/-90)$ skin and stiffener is weaker among all lamination angles. The central deflection for $(45/-45)$ skin and stiffener plate is 21.474 mm and for $(90/-90)$ skin and stiffener plate is 40.551 mm which is almost double of the previous result. The lamination scheme has great effect on the bending response of the stiffened plate.

3.3.2 Effect of stiffener depth

In this section the effect of stiffener depth on the bending response of the laminated composite stiffened plate will be analyzed. The depth of stiffener d_s will vary from 10 mm to 40 mm with an interval of 10 mm. The stacking in the stiffener is horizontal. The lamination scheme in the plate

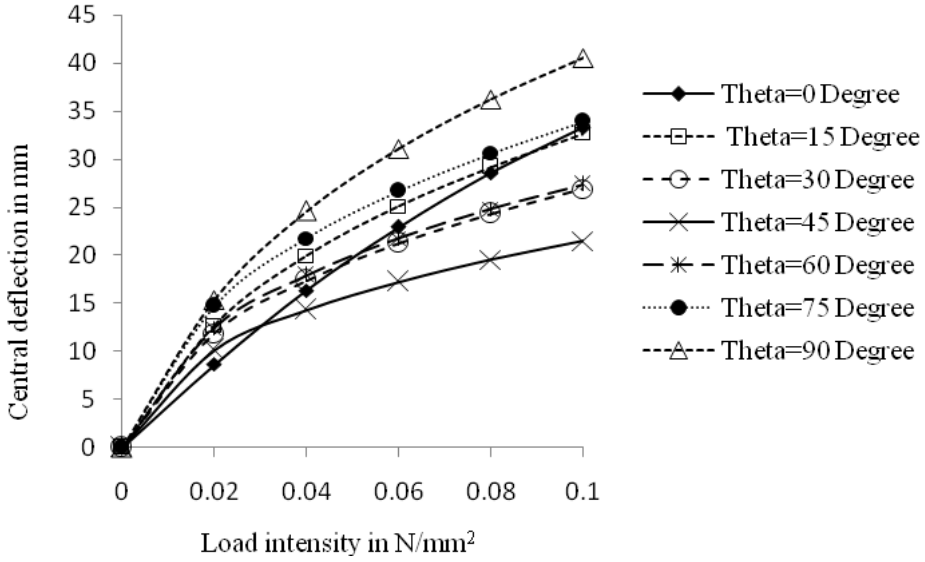

Fig. 10 Central deflection of stiffened plate for different angle of lamination

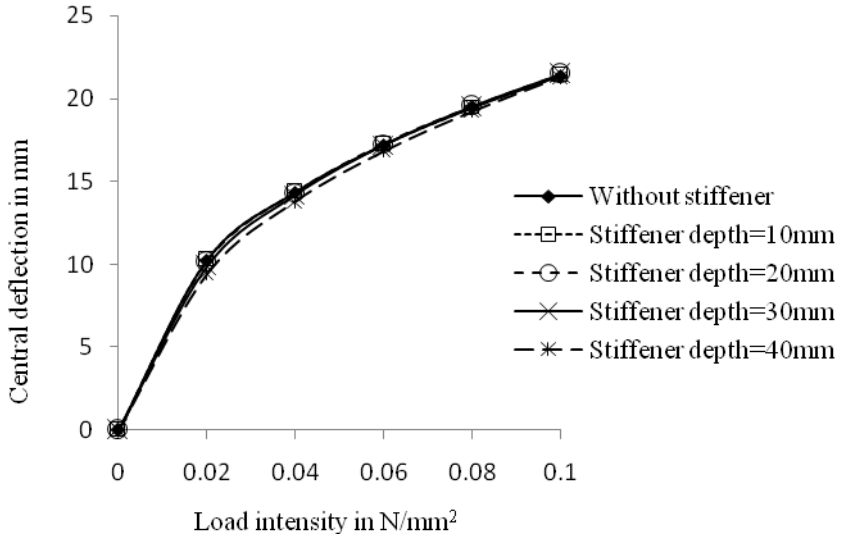

Fig. 11 Central deflection of stiffened plate for different depth of stiffener (nonlinear solution)

skin and stiffener is $(45/-45)$. The material constants are same as those of earlier section. The results of the central deflection with different load magnitude are shown in Fig. 11 along with the results of plate without stiffener. It is observed from this Fig. 11 that the effect of stiffener is not very much on the nonlinear bending of the laminated stiffened plate. This is because while performing the nonlinear solution the plate without stiffener is also showing very high stiffness value, which is coming from the stretching of the plate. In this high stiffness plate the contribution of the stiffener on the overall stiffness of the plate is not much. So the results are almost equal in

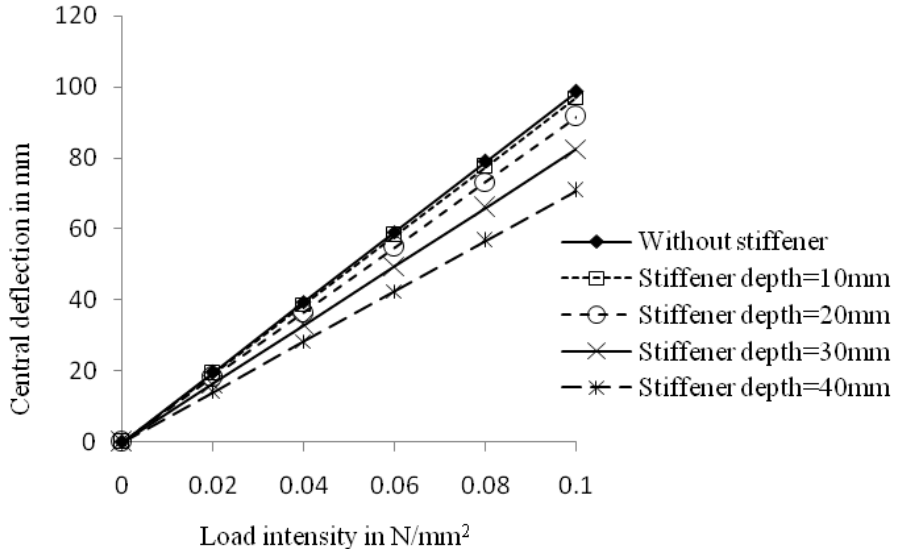

Fig. 12 Central deflection of stiffened plate for different depth of stiffener (linear solution)

all cases. On the other hand the contribution of stiffener can be remarkably observed on the bending behaviour of stiffened plate while performing a linear solution. In the linear solution the extra stiffness coming from the stretching effect of the plate is neglected. The results of the linear solution can be observed in Fig. 12.

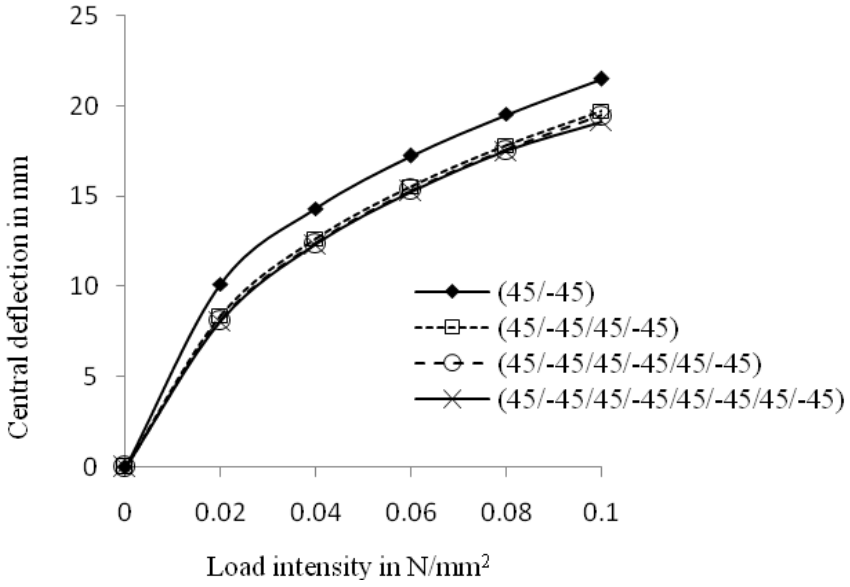

Fig. 13 Central deflection of stiffened plate for different numbers of layers in plate and stiffener

3.3.3 Effect of number of layers

To analyze the effect of number of layers in the plate and stiffener on the bending behaviour we have taken four different lamination scheme in the plate and stiffener. Those are (45/−45), (45/−45/45/−45), (45/−45/45/−45/45/−45) and (45/−45/45/−45/45/−45/45/−45) lamination on both plate and stiffener. The depth of stiffener d_s is 20 mm. The stacking in the stiffener is horizontal. The nonlinear bending results are shown in Fig. 13.

It is observed from the Fig. 13 that when the number of layers is increasing the plate is becoming more and more stiff.

4. Conclusions

The findings of the present investigation can be summarized as:

- The formulation of geometrically nonlinear analysis of laminated composite stiffened plate with Green-Lagrange strain displacement relationship in total Lagrangian co-ordinate is done. The formulation and analysis is implemented by writing a computer program in FORTRAN 90.
- The stiffened plate with (45/−45) skin and (45/−45) stiffener is stiffer among all lamination angles and with (90/−90) skin and (90/−90) stiffener is weaker among all lamination angles.
- The depth of stiffener is not showing much effect on the bending results of the plate. This is because in the nonlinear solution the plate without stiffener is also very highly stiff, due to the extra stiffness out of the stretching of the plate. In this high stiffness plate the contribution of the stiffener on the overall stiffness is not much.
- The number of layers, on the plate and stiffener for a given plate thickness and stiffener depth, has remarkable effect on the bending behaviour.
- The present formulation can be extended to nonlinear dynamic, postbuckling and other aspects of analysis of composite stiffened plates.

References

Ahmad, S., Irons, B.M. and Zienkiewicz, O.C. (1970), "Analysis of thick and thin shell structures by curved finite elements", *Int. J. Numer. Methods Eng.*, **2**(3), 419-451.

Almroth, B.O. and Brogan, F.A. (1978), The STAGS Computer Code, NASA CR-2950.

Bathe, K.J. (1996), *Finite Element Procedure*, Prentice-Hall of India Private Ltd., New Delhi, India.

Cetkovic, M. and Vuksanovic, Dj. (2011a), "Large deflection analysis of laminated composite plates using layerwise displacement model", *Struct. Eng. Mech., Int. J.*, **40**(2), 257-277.

Cetkovic, M and Vuksanovic, Dj. (2011b), "Geometric nonlinear analysis of laminated composite plates using layerwise displacement model", *J. Serb. Soc. Comput. Mech.*, **5**(1), 50-68.

Chattopadhyay, B., Sinha, P.K. and Mukhopadhyay, M. (1995), "Geometrically nonlinear analysis of composite stiffened plates using finite elements", *Compos. Struct.*, **31**(2), 107-118.

Chia, C.Y. (1988), "Geometrically nonlinear behaviour of composite plates – A review", *Appl. Mech. Rev.*, **41**(12), 439-450.

Dash, P. and Singh, B.N. (2010), "Geometrically nonlinear bending analysis of laminated composite plate", *Comm. Nonlin. Sci Num. Sim.*, **15**(10), 3170-3181.

Ferguson, G.H. and Clark, R.D. (1979), "A variable thickness curved beam and shell stiffener with sheat deformation", *Int. J. Num. Met. Eng.*, **14**, 581-592.

Goswami, S. and Mukhopadhyay, M. (1995), "Geometrically nonlinear analysis of laminated composite

stiffened shells", *J. Reinforced Plast. Compos.*, **14**(12), 1317-1336.
Hyer, M.W., Loap, D.C. and Starnes, J.H. (1990), "Stiffener/skin interactions in pressure-loaded composite panels", *AIAA J.*, **28**(3), 532-537.
Koko, T.S. and Olson, M.D. (1991), "Non-linear analysis of stiffened plates using super elements", *Int. J. Numer. Methods Eng.*, **31**(2), 319-343.
Kolli, M. and Chandrashekhara, K. (1997), "Nonlinear Static and dynamic analysis of stiffened laminated plates", *Int. J. Non-Linear Mech.*, **32**(1), 89-101.
Liao, C.L. and Reddy, J.N. (1990), "Analysis of anisotropic stiffened composite laminates using a continuum-based shell element", *Comput. Struct.*, **34**(6), 805-815.
Mukhopadhyay, M. and Satsangi, S.K. (1984), "Isoparametric stiffened plate bending element for the analysis of ships' structures", *Trans. RINA*, **126**, 144-151.
Ojeda, R., Prusty, B.G., Lawrence, N. and Thomas, G. (2007), "A new approach for the large deflection finite element analysis of isotropic and composite plates with arbitrary orientated stiffeners", *Finite Elem. Anal. Des.*, **43**(13), 989-1002.
Paik, J.K. and Lee, M.S. (2005), "A semi-analytical method for the elastic-plastic large deflection analysis of stiffened panels under combined biaxial compression/tension, biaxial in-plane bending, edge shear, and lateral pressure loads", *Thin-Wall. Struct.*, **43**(3), 375-410.
Polat, C. and Ulucan, Z. (2007), "Geometrically non-linear analysis of axisymmetric plates and shells", *Int. J. Sci. Technol.*, **2**(1), 33-40.
Rao, J.S. (1999), *Dynamics of Plates*, Narosa Publishing House, New Delhi, India.
Rao, D.V., Sheikh, A.H. and Mukhopadhyay, M. (1993), "A finite element large displacement analysis of stiffened plates", *Comput. Struct.*, **47**(6), 987-993.
Sapountzakis, E.J. and Dikaros, I.C. (2012a), "Large deflection analysis of plates stiffened by parallel beams with deformable connection", *J. Eng. Mech., ASCE*, **138**(8), 1021-1041.
Sapountzakis, E.J. and Dikaros, I.C. (2012b), "Large deflection analysis of plates stiffened by parallel beams", *Eng. Struct.*, **35**, 254-271.
Sheikh, A.H. and Mukhopadhyay, M. (2000), "Geometric nonlinear analysis of stiffened plates by the spline finite strip method", *Comput. Struct.*, **76**(6), 765-785.
Timoshenko, S.P. and Goodier, J.M. (1951), *Theory of Elasticity*, McGraw-Hill, Kogakusha.
Turvey, G.J. (1983), "Axisymmetric elastic large deflection behaviour of stiffened composite plates", *Compos. Struct.* 2, 72-88.
Wood, R.D. and Schrefler, B. (1978), "Geometrically nonlinear analysis-a correlation of finite element methods", *Int. J. Numer. Methods Eng.*, **12**(4), 635-642.
Zhang, Y.X. and Kim, K.S. (2006), "Geometrically nonlinear analysis of laminated composite plates by two new displacement-based quadrilateral plate elements", *Compos. Struct.*, **72**(3), 301-310.
Zienkiewicz, O.C. (1977), *The Finite Element Method*, Tata Mc-Graw Hill Publishing Company Ltd., New Delhi, India.

CC